AMERICAN SOCIETY FOR MICROBIOLOGY | Antimicrobial Agents and Chemotherapy®

PHARMACOLOGY

Simulating Intestinal Transporter and Enzyme Activity in a Physiologically Based Pharmacokinetic Model for Tenofovir Disoproxil Fumarate

Darren M. Moss,[a,b] Paul Domanico,[d] Melynda Watkins,[d] Seonghee Park,[c] Ryan Randolph,[c] Steve Wring,[c] Rajith Kumar Reddy Rajoli,[b] James Hobson,[b] Steve Rannard,[b] Marco Siccardi,[b] Andrew Owen[b]

School of Pharmacy, Keele University, Newcastle, United Kingdom[a]; Department of Molecular and Clinical Pharmacology, University of Liverpool, Liverpool, United Kingdom[b]; Scynexis, Durham, North Carolina, USA[c]; CHAI, Boston, Massachusetts, USA[d]

ABSTRACT Tenofovir disoproxil fumarate (TDF), a prodrug of tenofovir, has oral bioavailability (25%) limited by intestinal transport (P-glycoprotein), and intestinal degradation (carboxylesterase). However, the influence of luminal pancreatic enzymes is not fully understood. Physiologically based pharmacokinetic (PBPK) modeling has utility for estimating drug exposure from *in vitro* data. This study aimed to develop a PBPK model that included luminal enzyme activity to inform dose reduction strategies. TDF and tenofovir stability in porcine pancrelipase concentrations was assessed (0, 0.48, 4.8, 48, and 480 U/ml of lipase; 1 mM TDF; 37°C; 0 to 30 min). Samples were analyzed using mass spectrometry. TDF stability and permeation data allowed calculation of absorption rates within a human PBPK model to predict plasma exposure following 6 days of once-daily dosing with 300 mg of TDF. Regional absorption of drug was simulated across gut segments. TDF was degraded by pancrelipase (half-lives of 0.07 and 0.62 h using 480 and 48 U/ml, respectively). Previously reported maximum concentration (C_{max}; 335 ng/ml), time to C_{max} (T_{max}; 2.4 h), area under the concentration-time curve from 0 to 24 h (AUC_{0-24}; 3,045 ng · h/ml), and concentration at 24 h (C_{24}; 48.3 ng/ml) were all within a 0.5-fold difference from the simulated C_{max} (238 ng/ml), T_{max} (3 h), AUC_{0-24} (3,036 ng · h/ml), and C_{24} (42.7 ng/ml). Simulated TDF absorption was higher in duodenum and jejunum than in ileum ($p<0.05$). These data support that TDF absorption is limited by the action of intestinal lipases. Our results suggest that bioavailability may be improved by protection of drug from intestinal transporters and enzymes, for example, by coadministration of enzyme-inhibiting agents or nanoformulation strategies.

KEYWORDS tenofovir disoproxil fumarate, physiologically based pharmacokinetic modeling, HIV, bioavailability, HAART

Received 18 January 2017 **Returned for modification** 4 March 2017 **Accepted** 9 April 2017

Accepted manuscript posted online 17 April 2017

Citation Moss DM, Domanico P, Watkins M, Park S, Randolph R, Wring S, Rajoli RKR, Hobson J, Rannard S, Siccardi M, Owen A. 2017. Simulating intestinal transporter and enzyme activity in a physiologically based pharmacokinetic model for tenofovir disoproxil fumarate. Antimicrob Agents Chemother 61:e00105-17. https://doi.org/10.1128/AAC.00105-17.

Address correspondence to Darren M. Moss, d.moss1@keele.ac.uk.

Human immunodeficiency virus (HIV) is the cause of a currently incurable disease which constitutes a serious global health crisis. Oral antiretroviral therapy is the mainstay of current therapy and involves coadministration of drugs targeting multiple viral targets. Both drug-related adverse reactions and drug resistance have led to the development of newer antiretroviral drugs and drug classes. However, the cost and dosing schedule of treatments are a significant concern in low- and middle-income countries (L&MICs). Several effective antiretroviral drugs are now manufactured as generics and are marketed with significant cost savings to payers (1, 2).

Tenofovir disoproxil fumarate (TDF), a prodrug of tenofovir (TFV), is a cornerstone of first-line treatment in low-income and middle-income countries. TDF is a nucleotide

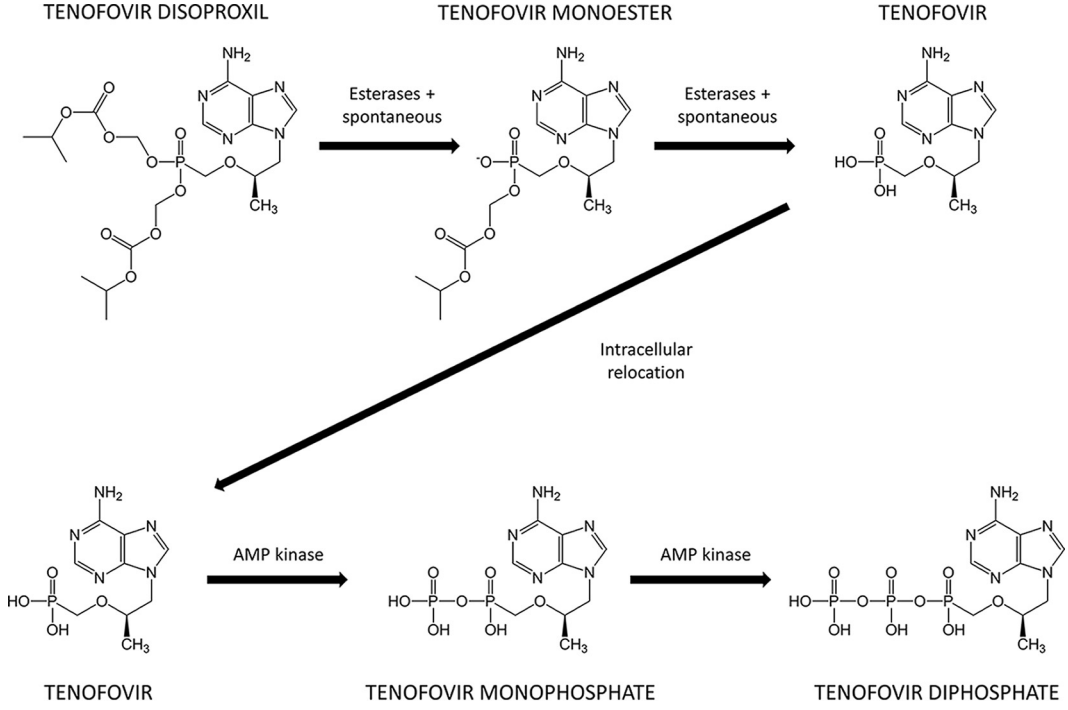

FIG 1 Process of converting the prodrug TDF to TFV and ultimately to the active substance TFV diphosphate.

reverse transcriptase inhibitor, which prevents viral DNA chain lengthening and replication (3) (Fig. 1). During preclinical development, TFV demonstrated low oral bioavailability (around 13%) (4), and TDF was developed to improve this by removing charged regions and increasing lipophilicity. However, the oral bioavailability of TDF was only moderately improved and is estimated at around 25% in fasted subjects (5, 6). Substantially improving the bioavailability of TDF would provide significant cost savings in L&MICs. In order to achieve this, it is important to understand the causes of low TDF bioavailability and to formulate potential targeting strategies.

Using Caco-2 cell monolayers as a model for the intestinal epithelial surface, the drug efflux transporter ABCB1 has been shown to readily transport TDF (7). As ABCB1 is involved in the elimination of substrates from the enterocytes of the intestine back into the luminal space, it is hypothesized that inhibitors of ABCB1 may improve TDF oral absorption. However, this ABCB1 inhibitory effect was not observed *in situ* using perfusion studies with rats (8). The significance of this finding is not clear due to the significantly faster TDF degradation in rat duodenal and ileal enterocytes than in corresponding human enterocytes (9).

Previous studies have investigated the impact of coadministered HIV protease inhibitors on TFV pharmacokinetics (7). Ritonavir-boosted protease inhibitors atazanavir, lopinavir, darunavir, and saquinavir all showed a modest increase in TFV exposure when coadministered with TDF. Protease inhibitors show various degrees of ABCB1 inhibition *in vitro*. Therefore, the same study also investigated the impact of these drugs on ABCB1-mediated transport of TDF. Darunavir, which in patients led to a 22% increase in TFV exposure, had no impact on TDF transport *in vitro*. In the case of the interactions observed with protease inhibitors and possibly other drugs, additional bioavailability-related mechanisms are likely to be involved alongside ABCB1.

TDF is rapidly metabolized to TFV in the presence of rat intestinal microsomes (8). It was hypothesized that carboxylesterase was responsible for this metabolism, and further investigations showed improved drug stability in the presence of certain natural fruit extracts and pharmacological esters. Protease inhibitors have shown various degrees of carboxylesterase inhibition, and this enzyme may therefore be involved in interactions between TDF and these drugs.

Pancreatic enzymes, including lipase, amylase, and trypsin, are released into the duodenum and are involved in the breakdown of ingested food in preparation for nutrient absorption. Pancreatic lipase is known to hydrolyze ester bonds (10), but the ability of lipase to metabolize TDF by ester-linked chain removal has not been previously investigated.

The initial aim of this study was to determine *in vitro* the extent of TDF metabolism by pancreatic lipase. These data were combined with previous information on TDF ABCB1-mediated transport and carboxylesterase metabolism to create a physiologically based pharmacokinetic (PBPK) model with informed absorption mechanisms involving all these processes. The model generated was then used to estimate the relative importance of these factors in TDF absorption, providing a platform to postulate possible dose reduction strategies.

RESULTS

Stability of TDF in pancrelipase. The breakdown of TDF was determined at various concentrations of lipase. The half-lives of TDF were determined as 4.0 min in 480 U/ml of lipase and 37.5 min in 48 U/ml of lipase. TDF was stable in 4.8 U/ml of lipase and below; therefore, half-life was not determined at these concentrations. Data were used to generate the following equation, relating lipase concentration to TDF stability, which was used to inform the PBPK model: $TDF_{1/2} = -0.0013 \times [\text{lipase}] + 0.6863$, where $TDF_{1/2}$ is the half-life of TDF (in hours) and [lipase] is the concentration of lipase in the intestine (in units per milliliter). To confirm the role of lipase in TDF degradation, selective inhibition of pancreatic enzymes was performed and the influence on TDF half-life was evaluated. Coincubation of TDF with lipase inhibitor orlistat resulted in a 33% increase in TDF half-life (16.0 min) compared to that with inhibitor-free incubation (12.0 min; $P = 0.02$), whereas no alteration in TDF half-life was observed with coincubation with the amylase inhibitor acarbose (12.6 min; $P = 0.66$) or trypsin inhibitor type 1-S from *Glycine max* (soybean) (12.7 min; $P = 0.23$).

Model verification. The 300-mg once-daily steady-state TFV pharmacokinetic study by Barditch-Crovo et al. showed variability in the median pharmacokinetic parameters maximum concentration (C_{max}), time to maximum concentration (T_{max}), and area under the concentration-time curve from 0 to 24 h (AUC_{0-24}) assessed between days 8, 15, and 35 of the study (6). Therefore, a mean and standard deviation (SD) between these assessment days were calculated and used for comparison with simulated data. The clinical C_{max} (335 ng ml^{-1}), T_{max} (2.4 h), and AUC_{0-24} (3,045 ng · h ml^{-1}) were all within a 0.5-fold difference of the simulated C_{max} (238 ng ml^{-1}; 0.41-fold higher), T_{max} (3 h; 0.2-fold lower), and AUC_{0-24} (3,036 ng · h ml^{-1}; 0-fold difference). The observed median TFV concentration at 24 h (C_{24}) following 7 days of once-daily oral dosing at 300 mg was 48.3 ng ml^{-1}, which was within the acceptable range of the median simulated TDF C_{24} of 42.7 ng ml^{-1} (Fig. 2A). The terminal plasma half-lives of TFV were determined as 11.7 h and 8.5 h from the median clinical and simulated pharmacokinetic data, respectively, following 7 days of 300-mg once-daily oral dosing. The simulated mean bioavailability of 300 mg of orally dosed TDF was 21.2% ± 3.3% (range, 13.1% to 27.6%). This estimation of oral bioavailability slightly underpredicted the 25% value estimated to be bioavailable from clinical studies. To validate the robustness of the model further, simulations were performed as described above but using alternative TDF oral dose sizes (75 mg, 150 mg, and 600 mg) and plasma concentration curves compared with previous clinical data (6). For the 75-mg TDF dose, the clinical C_{max} (53 ng ml^{-1}) and T_{max} (2.5 h) were within a 0.5-fold difference of the simulated C_{max} (51 ng ml^{-1}; 0.03-fold higher) and T_{max} (3 h; 0.2-fold lower) (Fig. 2B). The AUC_{0-24} and C_{24} for the 75-mg dose could not be determined from the clinical data, as TFV was undetectable at the 0- and 24-h time points on the plasma concentration curve. Therefore, clinical AUC_{1-12} (480 ng · h ml^{-1}) and C_{12} (34 ng ml^{-1}) were compared to simulated AUC_{1-12} (488 ng · h ml^{-1}; 0.02-fold lower) and C_{12} (28 ng ml^{-1}; 0.21-fold higher) (Fig. 2B). For the 150-mg TDF dose, the clinical C_{max} (135 ng ml^{-1}), T_{max} (2.5 h), AUC_{0-24} (1,581 ng · h ml^{-1}), and C_{24} (29 ng ml^{-1}) were all within a 0.5-fold difference of the

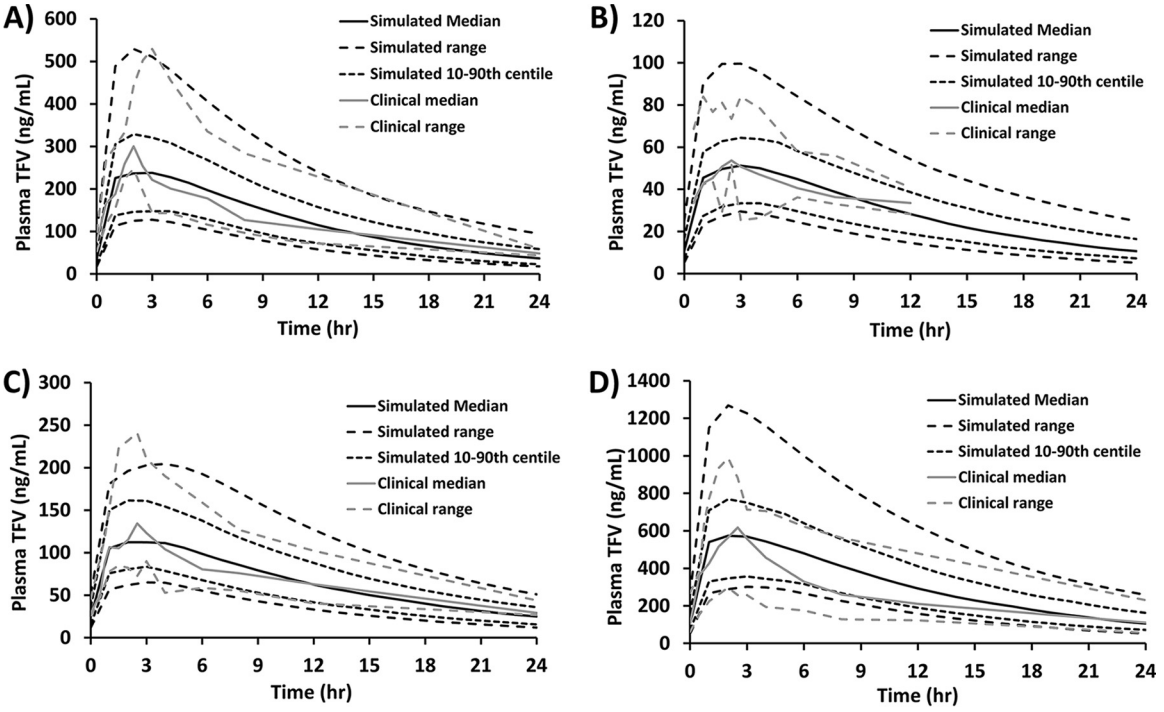

FIG 2 Validation of the physiologically based pharmacokinetic model strategy against clinical data of TDF once-daily, day 7 profiles for dose sizes of 300 mg (A), 75 mg (B), 150 mg (C), and 600 mg (D). Data are from reference 6.

simulated C_{max} (112 ng ml^{-1}; 0.21-fold higher), T_{max} (2 h; 0.25-fold higher), AUC_{0-24} (1,581 ng · h ml^{-1}; 0-fold difference), and C_{24} (23 ng ml^{-1}; 0.26-fold higher) (Fig. 2C). For the 600-mg TDF dose, the clinical C_{max} (618 ng ml^{-1}), T_{max} (2.5 h), AUC_{0-24} (6,166 ng · h ml^{-1}), and C_{24} (111 ng ml^{-1}) were all within a 0.5-fold difference of the simulated C_{max} (574 ng ml^{-1}; 0.08-fold higher), T_{max} (2 h; 0.25-fold higher), AUC_{0-24} (7,547 ng · h ml^{-1}; 0.18-fold lower), and C_{24} (106 ng ml^{-1}; 0.05-fold higher) (Fig. 2D).

Simulations of TDF and TFV fractional absorption. The regional intestinal absorption of TDF and TFV was simulated over 24 h in 100 virtual subjects following a single 300-mg oral dose of TDF (Fig. 3). The majority of drug entering the systemic

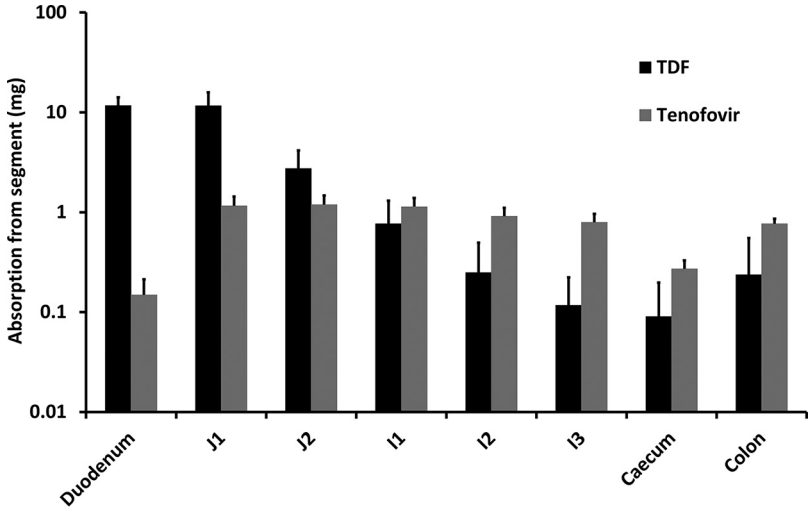

FIG 3 Amounts of TDF and tenofovir absorbed via each intestinal segment following a single 300-mg oral dose of TDF (mean ± SD 24 h postdose). J1, jejunum section 1; J2, jejunum section 2; I1, ileum section 1; I2, ileum section 2; I3, ileum section 3.

TABLE 1 Simulated median pharmacokinetic parameters of tenofovir following inhibition of factors involved in drug absorption of TDF[a]

Inhibited factor(s)	C_{max} (ng ml^{-1})	T_{max} (h)	AUC_{0-24} (ng · h ml^{-1})	C_{24} (ng ml^{-1})
None (control)	238	3	3,036	43
ABCB1	377	2	4,480	51
ABCB1 + CES	538	2	6,018	68
Lipase	1,013	3	12,873	199
ABCB1 + lipase	1,409	3	17,322	235
ABCB1 + CES + lipase	1,642	3	19,250	228

[a]Parameters were determined following 6 days of once-daily oral dosing of 300 mg of TDF in 100 healthy male subjects.

circulation was predicted to be accounted for by absorption of TDF directly, predominantly via the duodenum (11.7 mg) and section 1 of the jejunum (11.6 mg). Compared to absorption of TDF, overall absorption of TFV was predicted to be minor and varied from 0.15 mg in the duodenum to 1.19 mg in section 2 of the jejunum.

Simulations of tenofovir plasma concentrations following inhibition of intestinal ABCB1, carboxylesterase (CES), and luminal lipase. Data were found to be nonnormally distributed, so a Mann-Whitney U test was used to determine significance. The median tenofovir AUC_{0-24} (5th to 95th centile) of the control group (3,036 [1,752 to 4,762] ng · h ml^{-1}) was significantly less than those of the other groups following inhibition of ABCB1 (4,480 [2,538 to 7,228] ng · h ml^{-1}; $P < 0.01$), ABCB1 plus carboxylesterase (6,018 [3,514 to 10,976] ng · h ml^{-1}; $P < 0.01$), lipase (12,873 [9,020 to 20,827] ng · h ml^{-1}; $P < 0.01$), ABCB1 plus lipase (17,322 [12,752 to 26,226] ng · h ml^{-1}; $P < 0.01$), and ABCB1 plus carboxylesterase plus lipase (19,250 [14,215 to 29,208] ng · h ml^{-1}; $P < 0.01$) (Table 1).

Simulations of dose reduction strategies. Further simulations were performed in which the TDF dose was reduced in groups with inhibited factors, with the aim of achieving a median tenofovir AUC_{0-24} similar (within 10% difference) to that observed in the control group. Comparable tenofovir exposure was observed in all simulated groups following specific dose reductions in each case (Table 2). The median AUC_{0-24} (5th to 95th centile) following inhibition of ABCB1 (200-mg dose; 2,897 [1,678 to 4,603] ng · h ml^{-1}), ABCB1 plus carboxylesterase (150-mg dose; 3,002 [1,900 to 4,536] ng · h ml^{-1}), lipase (90-mg dose; 3,337 [2,245 to 5,341] ng · h ml^{-1}), ABCB1 plus lipase (60-mg dose; 3,279 [2,366 to 4,950] ng · h ml^{-1}), and ABCB1 plus carboxylesterase plus lipase (50-mg dose; 3,133 [2,286 to 4,751] ng · h ml^{-1}) were all within a 10% difference from that of the control group (3,036 [1,752 to 4,762] ng · h ml^{-1}).

DISCUSSION

In this study, we have established that TDF is unstable in the presence of physiologically relevant concentrations of pancrelipase. The most likely mechanism of this degradation is ester bond cleavage that first results in the TFV monoester and finally in TFV. As this process occurs in the luminal fluid prior to drug absorption, it is hypothesized that luminal lipase activity influences TDF bioavailability in humans. To investi-

TABLE 2 Dose reduction strategies following inhibition of factors involved in drug absorption of TDF[a]

Inhibited factor(s)	Dose size (mg)	AUC_{0-24} (ng · h ml^{-1})	% difference from control
None (control)	300	3,036	NA
ABCB1	200	2,897	−5
ABCB1 + CES	150	3,002	−1
Lipase	90	3,337	10
ABCB1 + lipase	60	3,279	8
ABCB1 + CES + lipase	50	3,133	3

[a]Parameters were determined following 6 days of once-daily oral dosing of TDF in 100 healthy male subjects. NA, not applicable.

gate this, the impact of luminal lipase was included in the PBPK model to estimate plasma TFV concentrations. Simulations suggest that the included factors contribute to the TFV exposure seen in subjects, with luminal lipase having a significant impact. In addition to results generated in this study, there is supporting evidence that lipase may be a relevant factor in determining TFV bioavailability. Protease inhibitors are able to inhibit lipase activity *in vitro* (11), and this process may be involved in the interactions seen between TDF and these drugs (possibly in addition to its known inhibition of transporters). Additionally, TDF exposure was increased 40% in human subjects when TDF was taken with a high-fat meal, whereas no comparable effect was seen with a low-fat meal (3). Although it is common to see improved biovavailability of highly lipophilic and insoluble drugs when they are taken with a fatty meal, TDF is reasonably soluble in intestinal fluid. Alternatively, it can be hypothesized that the increased fat in the intestinal fluid limits availability of lipase active sites for TDF metabolism. However, this competition has not been assessed and requires further empirical confirmation.

We have successfully employed PBPK modeling to include a variety of factors that influence TDF absorption. However, due to existing knowledge gaps and the complexities of biological processes involved in TFV pharmacokinetics, there are limitations to this approach, and it is important that these limitations are addressed. The simulations were undertaken assuming a population of fasted subjects, and the influence of ingested food and fats was not considered. This was due to incomplete information on the effects of food and fats on intestinal lipase activity and the influence of this on TDF stability. It was assumed that lipase was active only in the small intestine compartments and that the level of activity did not vary between these compartments in individual subjects. Per amount of enzyme, the activity levels of the lipase were assumed to be similar in both *in vitro* and *in vivo* environments, and in the *in vitro* experiments we used fasted simulated small intestinal fluid (FSSIF) to replicate the environment in fasted-state luminal fluid. Additionally, the use of porcine pancrelipase was chosen due to the well-characterized enzymatic activity of the product, where precise units of all enzymes (i.e., activities of lipase, amylase, and trypsin) per weight of substance were known, whereas human pancreatic fluids available to us did not provide the required information needed for utilization in the PBPK model. The distribution levels and activity levels of carboxylesterase protein in different sections of the intestine are unknown; therefore, it was assumed that the Caco-2 cell intestinal model was a suitable surrogate system.

Reformulation of TDF offers a strategy to improve bioavailability. There are cases in which multiple formulations of an antiretroviral are available, often for specific scenarios such as in pediatric treatment. Comparison studies have shown that formulation composition can significantly influence antiretroviral pharmacokinetics (1). Extended-release formulations have proven beneficial in many diseases and may have the potential to protect TDF from luminal enzymes. Inhibition of ABCB1 or carboxylesterase alone is unlikely to have a dramatic effect on TFV bioavailability, but a more holistic approach to inhibit multiple proteins (including lipase) may be more successful. This is somewhat supported by the modest increase in TFV exposure observed on coadministration with boosted protease inhibitors, and a more target-driven approach may achieve greater increases. Emerging nanotechnologies may also provide tailor-made opportunities to encapsulate and protect TDF from degradation until absorption is complete (12).

MATERIALS AND METHODS

Determination of TDF stability in pancrelipase. The stability of 1 mM TDF was assessed in triplicate in a range of lipase concentrations (0, 0.48, 4.8, 48, and 480 U/ml) using porcine pancrelipase. The medium used to perform experiments was fasted simulated small intestinal fluid (FSSIF; 3 mM sodium taurocholate, 0.2 mM lecithin, 34.8 mM sodium hydroxide, 68.62 mM sodium chloride, 19.12 mM maleic acid, 1 liter of deionized water, and hydrogen chloride added dropwise to achieve pH 6.5), and TDF concentrations were assessed at 0, 5, 10, 15, 20, and 30 min. Parallel experiments were performed to identify the specific enzymes involved in TDF degradation, where saturating concentrations of inhibitors of lipase (100 μg/ml of orlistat), amylase (1 mg/ml of acarbose), and trypsin (1 mg/ml of type 1-S trypsin inhibitor from soybean) (13) were coincubated with 20 μg/ml of TDF and alterations in TDF half-life were determined in the presence of a mix of porcine pancreatic enzymes (100 U/ml of lipase, 540 U/ml of

TABLE 3 Physiological factors relevant for simulating the oral absorption of TFV disoproxil and TFV in the PBPK model

Segment	pH	Vol (ml)	Radius (cm)	Transit time (h)	Absorption scaling
Stomach	1.3	46.56	NA[a]	0.25	×0
Duodenum	6	41.56	1.53	0.26	×1
Jejunum 1	6.2	154.2	1.45	0.93	×1
Jejunum 2	6.4	122.3	1.29	0.74	×1
Ileum 1	6.6	94.29	1.13	0.58	×1
Ileum 2	6.9	70.53	0.98	0.42	×1
Ileum 3	7.4	49.83	0.82	0.29	×1
Cecum	6.4	47.49	3.39	4.19	×1
Colon	6.8	50.33	2.41	12.57	×0.1

[a]NA, not applicable.

amylase, and 340 U/ml of trypsin). All experiments were performed at 37°C, and samples were processed and analyzed at Scynexis (Durham, NC) using liquid chromatography-tandem mass spectrometry (LC-MS/MS). The column used was a Synergi Polar RP column (2.0 by 150 mm; 4 μm; Phenomenex) kept at 60°C. Mobile phase A was 96% water–3% acetonitrile–1% acetic acid, and mobile phase B was 3% water–96% acetonitrile–1% acetic acid. The flow rate was 600 μl/min and consisted of 100% mobile phase A between 0 and 1 min, 2% mobile phase A–98% mobile phase B at 2 min, 2% mobile phase A–98% mobile phase B at 3 min, 100% mobile phase A at 3.1 min, and 100% mobile phase A at 4 min. TDF was detected in positive mode, Q1 mass was 520.1, and Q3 mass was 270 using collision energy 34. Labetalol was used as an internal standard.

Model construction. The PBPK model was created using SimBiology v.3.3, a product of Matlab v.8.2 (MathWorks, Natick, MA). The aim of the PBPK model was to simulate the steady-state pharmacokinetics of TFV in humans following 6 days of once-daily administration of 300 mg of TDF. In particular, the aspects potentially relevant to TDF absorption (solubility, lipase activity, carboxylesterase activity, and ABCB1 activity) were included to simulate the relative importance of each factor.

System parameters. The basic structure of the PBPK model is based on a previously published model created by us (14). Demographic factors of virtual male subjects between the ages of 18 and 60 (height, weight, body mass index, and body surface area) were taken from published literature and used in allometric equations to calculate individual organ volumes (15). The volume and rate of blood circulation in each simulated subject were calculated as previously described (14). The model was created with the following assumptions: (i) tissue compartments were treated as well-stirred compartments with instant distribution of drug, (ii) drug was not absorbed from the stomach compartment, (iii) the rate of drug absorption from the cecum and colon was reduced to 10-fold less than would be observed in the small intestine under the same conditions, and (iv) the model is blood flow limited. The physiological factors relevant for drug absorption in the intestinal compartments are based on the advanced compartmental absorption and transit (ACAT) model and are given in Table 3 (16).

Drug parameters. (i) Solubility of TDF in the luminal fluid. In order to account for potential solubility-induced absorption limitations, the solubility of TDF was measured by Corealis Pharma (Quebec, Canada) in a physiologically relevant range of buffered pH solutions. Solubility of TDF was high at 9,300, 4,800, and 6,200 mg/liter in buffered solutions of pHs 2, 4.5, and 8, respectively. These results were then used to derive the following quadratic equation to calculate the pH-dependent limitations to TDF luminal solubility (in milligrams per liter) in the PBPK model intestinal compartments: TDFs = (366.67 × [IpH]^2) – (4,183.33 × IpH) + 16,200, where TDFs is the maximum possible solubility of TDF (in milligrams per liter) and IpH is the pH of the intestinal segment fluid.

Only soluble TDF, which was continually determined throughout simulations in each intestinal segment, was available for absorption in the PBPK absorption model.

(ii) Stability of TDF in the luminal fluid. Intestinal lipase concentrations were acquired from the literature and included in the small intestine segments of the PBPK model (duodenum, jejunum, and ileum) (17). Each simulated fasted subject was given a physiologically relevant concentration of luminal lipase which was randomly assigned within the ranges obtained from published literature of between 100 and 400 U/ml. Using the *in vitro* metabolism data generated in this study, an equation was then developed establishing the relationship between lipase concentration and drug half-life, as given in Results. The lipase-dependent rate of elimination was then determined for each simulated subject and the degraded TDF was assumed to be converted to TFV, which either is absorbed or passes along and out of the intestine, as detailed below.

(iii) Absorption of TDF and TFV. TDF permeation through a Caco-2 cell monolayer has been previously investigated, and the apparent permeability (P_{app}) was found to be drug concentration dependent (7). The authors hypothesized that this was the result of active transport saturation (specifically, saturation of ABCB1) when higher TDF concentrations were added to the receiver compartment. To inform the current model of this scenario, this relationship between TDF concentrations and P_{app} was continuously redetermined in each intestinal segment using the following polynomial equation, derived from a previous study (7): $TDF_{Papp} = -1.9 \times 10^{-26} \times [TDF_{conc}]^6 + 3.3 \times 10^{-22} \times [TDF_{conc}]^5 - 2.2 \times 10^{-18} \times [TDF_{conc}]^4 + 7.5 \times 10^{-15} \times [TDF_{conc}]^3 - 1.3 \times 10^{-11} \times [TDF_{conc}]^2 + 1.1 \times 10^{-8} \times [TDF_{conc}] + 1.6 \times 10^{-7}$,

where TDF_{Papp} is the estimated TDF P_{app} value at a specific concentration of TDF and TDF_{conc} is the concentration of TDF.

Using previously established equations, P_{app} was used to generate the rate of drug absorption in the model (18, 19). Intestinal absorption of TFV, the breakdown product of TDF occurring via luminal lipase, was included. The rate of intestinal TFV absorption was determined by scaling the P_{app} value of 0.41 cm $\times$ 10^{-6} s^{-1} determined previously in MDCK monolayers (20, 21).

(iv) Distribution of TFV. The volume of distribution of TFV was simulated considering the volume of distribution of 0.813 liter/kg described in population pharmacokinetic studies (22), and the tissue distribution was determined using previously published equations (23, 24).

(v) Clearance of TFV. TFV is predominantly eliminated from the body unchanged via the kidneys. In order to account for this loss, clearance of TFV was included in the model. The multiple physiological factors involved in the elimination of TFV, such as the effect of drug transporters and tubular reabsorption, have not been fully characterized, making a mechanistic prediction of TFV renal elimination difficult. Therefore, a TFV total clearance rate of 0.066 liter/h/kg was derived from a previous population pharmacokinetic study and was included in our model (6).

Model verification. To verify the model, pharmacokinetic data from simulations were compared to clinical data. Following 6 days of once-daily dosing of 300 mg of TDF in 100 simulated subjects, median TFV C_{max}, T_{max}, AUC_{0-24}, and C_{24} were calculated and contrasted to steady-state pharmacokinetics observed in real subjects, taken from a randomized, double-blind, placebo-controlled, escalating-dose study of four doses (75, 150, 300, and 600 mg given once daily) with 8 or 9 subjects in each group (6). Additionally, the terminal plasma half-life of TDF was estimated from simulated concentration plots and compared to the half-life generated from clinical data. The bioavailability of orally administered TDF is estimated at around 25% of the total dose (25), and the bioavailability of 300 mg of orally administered TDF was determined from our simulations (mean $\pm$ standard deviation, with minimum and maximum range) as a comparison to further validate the model. As a predetermined measure of success for the model validation, a 0.5-fold difference or less between clinical and predicted pharmacokinetic parameters was deemed acceptably accurate (26, 27). Pharmacokinetic parameters were determined by noncompartmental analysis using PK Solutions 2.0 (Summit Research Services, UK).

To validate the robustness of the model further, simulations were performed as described above but using alternative TDF oral dose sizes (75 mg, 150 mg, and 600 mg). Pharmacokinetic parameters (median TFV C_{max}, T_{max}, AUC_{0-24}, and C_{24}) were generated from these simulations and were compared to available clinical pharmacokinetic data where these dose sizes were utilized (6).

Assessment of regional absorption of TDF and TFV. The regional absorption of TDF and TFV was simulated in 100 virtual subjects following a single 300-mg oral dose of TDF. Mean absorption amounts (in milligrams) with standard deviations were determined 24 h postdose in duodenum, jejunum section 1 (j1), jejunum section 2 (j2), ileum section 1 (i1), ileum section 2 (i2), ileum section 3 (i3), cecum, and colon (Table 3).

Prediction of TFV pharmacokinetics following inhibition of factors involved in absorption. In order to determine the influence of intestinal ABCB1, CES, and lipase on tenofovir exposure, each factor was individually (with the exception of CES) and in combination removed from simulations and the pharmacokinetics of TFV were determined for each combination. In the case where lipase activity in the model was eliminated, simulations were performed where the intestinal $TDF_{1/2}$ was 0 min. In the case where ABCB1 activity was inhibited, simulations were performed using a TDF P_{app} value of 3.6 cm $\times$ 10^{-6} s^{-1}, taken from a previous study (7). In the case where ABCB1 and CES activities in the model were inhibited, simulations were performed using a TDF P_{app} value of 9.41 cm $\times$ 10^{-6} s^{-1}, taken from a previous Caco-2 cell permeation study in which inhibition of ABCB1 and CES activity was achieved using TPGS (ABCB1 inhibitor) and 1 mM propylparaben (CES inhibitor) (7, 20). In each group, mean tenofovir C_{max}, T_{max}, AUC_{0-24}, and C_{24} were calculated following 6 days of once-daily dosing with 300 mg of TDF in 100 simulated subjects.

ACKNOWLEDGMENTS

We thank the Bill and Melinda Gates Foundation and the Department for International Development for funding this work.

We have no conflict of interest to declare.

REFERENCES

1. Bastiaans DE, Cressey TR, Vromans H, Burger DM. 2014. The role of formulation on the pharmacokinetics of antiretroviral drugs. Expert Opin Drug Metab Toxicol 10:1019–1037. https://doi.org/10.1517/17425255.2014.925879.
2. Pinheiro Edos S, Bruning K, Macedo MF, Siani AC. 2014. Production of antiretroviral drugs in middle- and low-income countries. Antivir Ther 19(Suppl 3):S49–S55.
3. Kearney BP, Flaherty JF, Shah J. 2004. Tenofovir disoproxil fumarate—clinical pharmacology and pharmacokinetics. Clin Pharmacokinet 43:595–612. https://doi.org/10.2165/00003088-200443090-00003.
4. Deeks SG, Barditch-Crovo P, Lietman PS, Hwang F, Cundy KC, Rooney JF, Hellmann NS, Safrin S, Kahn JO. 1998. Safety, pharmacokinetics, and antiretroviral activity of intravenous 9-[2-(R)-(phosphonomethoxy)propyl]adenine, a novel anti-human immunodeficiency virus (HIV) therapy, in HIV-infected adults. Antimicrob Agents Chemother 42:2380–2384.
5. Shaw JP, Sueoko CM, Oliyai R, Lee WA, Arimilli MN, Kim CU, Cundy KC. 1997. Metabolism and pharmacokinetics of novel oral prodrugs of 9-[(R)-2-(phosphonomethoxy)propyl]adenine (PMPA) in dogs. Pharm Res 14:1824–1829. https://doi.org/10.1023/A:1012108719462.
6. Barditch-Crovo P, Deeks SG, Collier A, Safrin S, Coakley DF, Miller M, Kearney BP, Coleman RL, Lamy PD, Kahn JO, McGowan I, Lietman PS. 2001. Phase I/II trial of the pharmacokinetics, safety, and antiretroviral activity of tenofovir disoproxil fumarate in human immunodeficiency

virus-infected adults. Antimicrob Agents Chemother 45:2733–2739. https://doi.org/10.1128/AAC.45.10.2733-2739.2001.
7. Tong L, Phan TK, Robinson KL, Babusis D, Strab R, Bhoopathy S, Hidalgo IJ, Rhodes GR, Ray AS. 2007. Effects of human immunodeficiency virus protease inhibitors on the intestinal absorption of tenofovir disoproxil fumarate in vitro. Antimicrob Agents Chemother 51:3498–3504. https://doi.org/10.1128/AAC.00671-07.
8. van Gelder J, Deferme S, Naesens L, De Clercq E, van den Mooter G, Kinget R, Augustijns P. 2002. Intestinal absorption enhancement of the ester prodrug tenofovir disoproxil fumarate through modulation of the biochemical barrier by defined ester mixtures. Drug Metab Dispos 30:924–930. https://doi.org/10.1124/dmd.30.8.924.
9. Van Gelder J, Shafiee M, De Clercq E, Penninckx F, Van den Mooter G, Kinget R, Augustijns P. 2000. Species-dependent and site-specific intestinal metabolism of ester prodrugs. Int J Pharm 205:93–100. https://doi.org/10.1016/S0378-5173(00)00507-X.
10. Chen Q, Sternby B, Nilsson A. 1989. Hydrolysis of triacylglycerol arachidonic and linoleic acid ester bonds by human pancreatic lipase and carboxyl ester lipase. Biochim Biophys Acta 1004:372–385. https://doi.org/10.1016/0005-2760(89)90086-6.
11. Wignot TM, Stewart RP, Schray KJ, Das S, Sipos T. 2004. In vitro studies of the effects of HAART drugs and excipients on activity of digestive enzymes. Pharm Res 21:420–427. https://doi.org/10.1023/B:PHAM.0000019294.03188.cf.
12. Moss DM, Siccardi M. 2014. Optimizing nanomedicine pharmacokinetics using physiologically based pharmacokinetics modelling. Br J Pharmacol 171:3963–3979. https://doi.org/10.1111/bph.12604.
13. Guillamon E, Pedrosa MM, Burbano C, Cuadrado C, Sanchez MDC, Muzquiz M. 2008. The trypsin inhibitors present in seed of different grain legume species and cultivar. Food Chem 107:68–74. https://doi.org/10.1016/j.foodchem.2007.07.029.
14. Rajoli RK, Back DJ, Rannard S, Freel Meyers CL, Flexner C, Owen A, Siccardi M. 2015. Physiologically based pharmacokinetic modelling to inform development of intramuscular long-acting nanoformulations for HIV. Clin Pharmacokinet 54:639–650. https://doi.org/10.1007/s40262-014-0227-1.
15. Bosgra S, Eijkeren Jv, Bos P, Zeilmaker M, Slob W. 2012. An improved model to predict physiologically based model parameters and their inter-individual variability from anthropometry. Crit Rev Toxicol 42:751–767. https://doi.org/10.3109/10408444.2012.709225.
16. Heikkinen AT, Baneyx G, Caruso A, Parrott N. 2012. Application of PBPK modeling to predict human intestinal metabolism of CYP3A substrates—an evaluation and case study using GastroPlus. Eur J Pharm Sci 47:375–386. https://doi.org/10.1016/j.ejps.2012.06.013.
17. McConnell EL, Fadda HM, Basit AW. 2008. Gut instincts: explorations in intestinal physiology and drug delivery. Int J Pharm 364:213–226. https://doi.org/10.1016/j.ijpharm.2008.05.012.
18. Sun D, Lennernas H, Welage LS, Barnett JL, Landowski CP, Foster D, Fleisher D, Lee KD, Amidon GL. 2002. Comparison of human duodenum and Caco-2 gene expression profiles for 12,000 gene sequences tags and correlation with permeability of 26 drugs. Pharm Res 19:1400–1416. https://doi.org/10.1023/A:1020483911355.
19. Yu LX, Amidon GL. 1999. A compartmental absorption and transit model for estimating oral drug absorption. Int J Pharm 186:119–125. https://doi.org/10.1016/S0378-5173(99)00147-7.
20. Watkins ME, Wring S, Randolph R, Park S, Powell K, Lutz L, Nowakowski M, Ramabhadran R, Domanico PL. 2017. Development of a novel formulation that improves preclinical bioavailability of tenofovir disoproxil fumarate. J Pharm Sci 106:906–919. https://doi.org/10.1016/j.xphs.2016.12.003.
21. Gertz M, Harrison A, Houston JB, Galetin A. 2010. Prediction of human intestinal first-pass metabolism of 25 CYP3A substrates from in vitro clearance and permeability data. Drug Metab Dispos 38:1147–1158. https://doi.org/10.1124/dmd.110.032649.
22. Fung HB, Stone EA, Piacenti FJ. 2002. Tenofovir disoproxil fumarate: a nucleotide reverse transcriptase inhibitor for the treatment of HIV infection. Clin Ther 24:1515–1548. https://doi.org/10.1016/S0149-2918(02)80058-3.
23. Poulin P, Theil FP. 2002. Prediction of pharmacokinetics prior to in vivo studies. 1. Mechanism-based prediction of volume of distribution. J Pharm Sci 91:129–156.
24. Peters SA. 2008. Evaluation of a generic physiologically based pharmacokinetic model for lineshape analysis. Clin Pharmacokinet 47:261–275. https://doi.org/10.2165/00003088-200847040-00004.
25. Gallant JE, Deresinski S. 2003. Tenofovir disoproxil fumarate. Clin Infect Dis 37:944–950. https://doi.org/10.1086/378068.
26. Abduljalil K, Cain T, Humphries H, Rostami-Hodjegan A. 2014. Deciding on success criteria for predictability of pharmacokinetic parameters from in vitro studies: an analysis based on in vivo observations. Drug Metab Dispos 42:1478–1484. https://doi.org/10.1124/dmd.114.058099.
27. Sager JE, Yu J, Ragueneau-Majlessi I, Isoherranen N. 2015. Physiologically based pharmacokinetic (PBPK) modeling and simulation approaches: a systematic review of published models, applications, and model verification. Drug Metab Dispos 43:1823–1837. https://doi.org/10.1124/dmd.115.065920.